Glucose and Fructose Hydrates in Aqueous Solution by IR Spectroscopy

Jean-Joseph Max[†] and Camille Chapados*

Département de chimie-biologie, Université du Québec à Trois-Rivières, Trois-Rivières, QC, Canada G9A 5H7

Received: October 20, 2006; In Final Form: January 26, 2007

In the mid-infrared attenuated total reflectance (MIR−ATR) spectra of aqueous D-glucose and D-fructose solutions, two hydrates were found by factor analysis (FA) for each sugar, D-glucose penta- and dihydrates and D-fructose penta- and monohydrates. We obtained the spectra and abundances for these hydrates as a function of carbohydrate concentrations. The biggest difference in these spectra lies in the CO stretch region. From the distribution of the species, the equilibrium between D-glucose pentahydrate and dihydrate is $3(H_2O)_2 + 2(C_6H_{12}O_6{\cdot}2H_2O) \rightleftarrows 2(C_6H_{12}O_6{\cdot}5H_2O)$, with the equilibrium constant $K_G = (3.2 \pm 0.6) \times 10^{-5}$ L^3 mol^{-3}. For D-fructose, the equilibrium is between pentahydrate and monohydrate, $2(H_2O)_2 + C_6H_{12}O_6{\cdot}H_2O \rightleftarrows C_6H_{12}O_6{\cdot}5H_2O$, with the equilibrium constant $K_F = (7.1 \pm 1.2) \times 10^{-3}$ L^2 mol^{-2}. The four hydrates are present only in aqueous solutions and cannot be obtained in the solid state.

1. Introduction

Carbohydrates are an important class of compounds with the general formula $C_x(H_2O)_y$ that includes sugars, starch, and cellulose. They are important commercial products used in food products for humans and animals and are increasingly being transformed as fuel for vehicles. The product of cane sugar is sucrose, which is a primary product in the food industry. The first step in the hydrolysis of sucrose is glucose and fructose. Since the hydrolysis of these sugars involves water, we wanted to know the nature of the relation of water with these sugars in the aqueous solutions because the principal reactions of these sugars are in that medium. Furthermore, glucose is one of the primary fuels in the body that liberates energy when it is broken down into carbon dioxide and water. This process is done in an aqueous medium. Pure crystalline sugars are stable products, but their use is mostly in aqueous form where they interact with water to form hydrates. Although they have been studied since the 1920s,[1−3] their composition is not completely determined. A few years ago, we started to reexamine the hydrates of aqueous carbohydrates by mid-infrared (MIR) spectroscopy since this technique is a multispectral technique that is very sensitive to OH groups and the hydrogen bonds they make. We started with sucrose ($C_{12}H_{22}O_{11}$) since it is one of the principal commercial carbohydrate products. In that paper (hereinafter I) published on sucrose hydrates in water by IR spectroscopy, we determined, with the use of factor analysis (FA), that in aqueous solutions two hydrates are present in the entire solubility range of the sugar.[4] We obtained the hydrates' real spectra and abundances as a function of the sucrose concentration. The two species are the sucrose pentahydrate and dihydrate, related by the equation $3H_2O + C_{12}H_{22}O_{11}{\cdot}2H_2O \rightleftarrows C_{12}H_{22}O_{11}{\cdot}5H_2O$ and its equilibrium constant $K_e = (4.1 \pm 0.3) \times 10^{-5}$ L^3 mol^{-3}. While the two hydrates are present in the whole solubility range of the sugar, the first one is more abundant in the lower concentration range, and the second is more abundant in the higher concentration range. The addition of the two concentration species gave a linear relationship as a function of the prepared concentrations in the whole sucrose solubility range, whereas the use of the concentration of only one sucrose species gave a linear relationship only in a limited concentration range.[5−8]

The principal spectral differences between the two hydrates lie in the C−O stretch region (around 1050 cm^{-1}). The hydrate species are found only in solution. Consequently, drying the solutions will destroy the hydrates. For more details on the sucrose hydrates, one should consult I and the references therein. Recently, infrared was used to determine the sugar content of plant cultivars.[9] The various uptake rates of different combinations of glucose, fructose, and sucrose could easily be followed with this simple and rapid technique. As in I, this paper shows the usefulness of the IR technique in monitoring the sugar content in different systems. Moreover, in I, we showed that the real spectra of the species can be obtained, from which structural information can be retrieved.

The first step in the hydrolysis of sucrose gives glucose and fructose, two important commodities and biologically important carbohydrates. Although the literature on these sugars is abundant, principally on glucose, none of the papers were done in the same orientation as our sucrose paper (I) that dealt with sucrose solvated species in aqueous solutions. The purpose of the present study is to fill this gap by analyzing the MIR spectra of aqueous D-glucose and D-fructose solutions over their entire solubility range. Specifically, we want to determine (i) the number of hydrates present in the solutions, (ii) the species abundances as a function of sugar concentration, (iii) the MIR spectra of the sucrose hydrates, (iv) the molecular composition of the hydrates, and (v) the equilibrium constant between the hydrates.

2. Experimental Methods and Data Analysis

2.1. Chemicals and Solutions. The D-glucose (Aldrich Chemical Co., A.C.S. reagent [50-99-7], purity >99%, water content <0.2%, FW 180.16) and D-fructose (Aldrich Chemical Co., A.C.S. [57-48-7], purity >99%, water content <0.2%, FW 180.16) were used without further purification. Deionized water

* To whom correspondence should be addressed. E-mail: Camille.Chapados@uqtr.ca.

† Current address: ITF Labs, 400 Montpellier, Montreal, (QC), Canada H4N 2G7. E-mail: jjmax@itfoptical.com.

10.1021/jp066882r CCC: $37.00
Published on Web 03/17/2007

TABLE 1: Parameter of the Experimental Aqueous Glucose and Fructose Mixtures (FW ($C_6H_{12}O_6$) = 180.20)

Sample Composition				MFs		
D-Glucose			Water	Water	Pentahydrate	Dihydrate
g added to 25 mL of water	mol × L^{-1}[a]	mol fraction	mol × L^{-1}	mol × L^{-1}	mol × L^{-1}	mol × L^{-1}
0.000	−0.001	0.000	55.341	55.341	0.000	0.000
0.015	0.003	0.001	55.322	55.322	0.003	0.001
0.078	0.017	0.003	55.238	55.180	0.013	0.004
0.208	0.046	0.008	55.067	54.915	0.032	0.013
0.503	0.110	0.020	54.680	54.258	0.076	0.033
1.019	0.221	0.039	54.014	53.145	0.154	0.069
2.030	0.430	0.075	52.743	51.139	0.286	0.141
3.981	0.805	0.138	50.422	47.430	0.518	0.289
6.970	1.319	0.219	47.189	41.716	0.777	0.523
11.028	1.919	0.307	43.368	35.848	1.041	0.855
16.060	2.541	0.392	39.391	30.584	1.243	1.303
23.259	3.254	0.483	34.833	24.360	1.338	1.933
30.323	3.809	0.549	31.310	19.817	1.294	2.539
36.561	4.211	0.595	28.772	16.790	1.176	3.037
40.676	4.440	0.620	27.327	15.292	1.068	3.356

D-Fructose			Water	Water	Pentahydrate	Monohydrate
g added to 25 mL of water	mol × L^{-1}[a]	mol fraction	mol × L^{-1}	mol × L^{-1}	mol × L^{-1}	mol × L^{-1}
0.000	0.000	0.000	55.309	55.309	0.000	0.000
0.010	0.002	0.000	55.296	55.215	−0.001	0.002
0.036	0.008	0.001	55.263	55.101	0.001	0.004
0.080	0.018	0.003	55.207	54.890	0.005	0.010
0.154	0.034	0.006	55.112	54.742	0.020	0.009
0.263	0.058	0.010	54.974	54.406	0.039	0.012
0.554	0.121	0.022	54.606	53.589	0.090	0.021
1.053	0.228	0.041	53.981	52.384	0.177	0.035
2.069	0.438	0.077	52.739	50.278	0.338	0.069
4.082	0.825	0.141	50.398	46.333	0.630	0.160
7.126	1.347	0.222	47.163	41.357	0.988	0.326
11.138	1.940	0.309	43.424	36.121	1.318	0.614
16.141	2.560	0.393	39.479	30.511	1.566	1.005
22.234	3.177	0.471	35.533	25.383	1.708	1.508
28.298	3.680	0.532	32.325	21.625	1.706	2.027
34.355	4.097	0.580	29.666	18.764	1.614	2.519
40.385	4.448	0.618	27.436	16.503	1.526	2.971
46.438	4.749	0.651	25.528	15.237	1.319	3.456
52.469	5.009	0.678	23.890	14.119	1.174	3.827

[a] Ref 30.

was used to prepare the aqueous solutions that cover the entire solubility range. The sample compositions are given in Table 1.

2.2. IR Measurements. The IR measurements were obtained using a model 510P Nicolet FT−IR spectrometer with a DTGS detector. Two KBr windows isolated the measurement chamber from the outside. The samples were contained in a Macro Circle cell (SpectraTech, Inc., Part number 0005-001) equipped with a ZnSe crystal rod (8 cm long) in an ATR configuration (the beam is incident at an angle of 45° with the rod's axis and makes 11 internal reflections) from which nearly 3.3 of them were in contact with the liquid sample.[10] The spectral range of this system is 5500 to 650 cm^{-1}. The spectra were taken under nitrogen flow to ensure low CO_2 and water vapor in the spectrometer. Each spectrum represents an accumulation of 500 scans at 2 cm^{-1} resolution (0.965 cm^{-1} sampling interval). The measurements were made at 27.1 ± 0.3 °C. The cell was carefully dried before each series of measurements. Model 510P being a single-beam spectrometer, a background reference was taken with the cell empty before measuring the spectra of each series of samples. These were obtained by circulating the liquid mixture into the cell (approximately 1 mL volume) at a rate of 1.1 mL min^{-1}.

The IR measurements consisted of obtaining the ATR background and sample interferograms. These were transformed into spectral intensities R_0 and R, respectively. The ratio of R/R_0 is the intensity I for the spectral range being studied. Thereafter, the 5029 data points $\{I(\tilde{\nu})$ vs $\tilde{\nu}$ (in cm^{-1})$\}$ of each spectrum were transferred to a spreadsheet program for numerical analysis. The intensities I were transformed into absorbance units, log-(1/I) (abbreviated in some cases as AU). A small baseline shift (less than 0.004 AU) was necessary to obtain a null mean absorbance in the 5500−5400 cm^{-1} region where water,[11] D-glucose, and D-fructose do not absorb. The second derivatives used to determine the band maxima were calculated by the Savitzky and Golay method[12] with a moving quadratic−cubic polynomial fitting. The number of points in the moving average varied for the different spectral regions to give the best enhancement.

2.3. Factor Analysis (FA). *2.3.1. Determination of the Minimum Number of Principal Factors.* Factor analysis (FA) of a spectral data set is a process by which the principal species of a mixture can be identified and their concentrations obtained through calibration of derived multiplying factors (MFs). Several mathematical methods using matrix multiplication can lead to the principal factors.[13−15] However, most methods give abstract factors that are not easy to interpret at the molecular level.[13,14]

We recently developed an effective method to evaluate the MFs of a spectral set relative to a given subset of principal

factors. Essentially, it consists of the following steps. The first one in FA is to determine the number of principal factors in the set.[14] FA is applied to a set of n experimental spectra, S^e, of carbohydrate−water solutions of length l $(\mathbf{S^e})_{l,n}$. A subset of f experimental spectra is used in the determination of the minimum number, f, of principal spectra S^P of the same length l $(\mathbf{S^P})_{l,f}$. The MFs are the abundance of each $\mathbf{S^P}$ at a given concentration, $(\mathbf{MF})_{f,n}$. The product of the two terms must reproduce the entire set of experimental spectra. That is

$$(\mathbf{S^e})_{l,n} = (\mathbf{S^P})_{l,f} \times (\mathbf{MF})_{f,n} + (\mathbf{R^e})_{l,n} \quad (1)$$

where $(\mathbf{R^e})_{l,n}$ represents the matrix of the difference spectra (residues). From eq 1, the MFs are easily obtained with the following equation (see Appendix)

$$(\mathbf{MF})_{f,n} = [(\mathbf{S^P})^{\mathrm{T}}_{f,l} \times (\mathbf{S^P})_{l,f}]^{-1} \times (\mathbf{S^P})^{\mathrm{T}}_{f,l} \times (\mathbf{S^e})_{l,n} \quad (2)$$

The validity of MFs obtained through eq 2 is subject to the following condition

$$(\mathbf{S^P})^{\mathrm{T}}_{f,l} \times (\mathbf{R^e})_{l,n} \cong 0 \quad (3)$$

Since the scalar product is a very simple calculation, eqs 2 and 3 were applied using a spreadsheet program that can provide small matrix multiplication and inversion. Equation 2 involves two relatively small matrices ($f \times f$ and $f \times n$, respectively) that contain the scalar products of the principal factor spectra together, $(\mathbf{S^P})^{\mathrm{T}}_{f,l} \times (\mathbf{S^P})_{l,f}$ and principal factor spectra with experimental spectra $(\mathbf{S^P})^{\mathrm{T}}_{f,l} \times (\mathbf{S^e})_{l,n}$. The elements of these two matrices are easy to obtain using a spreadsheet program. Therefore, results were obtained without any algorithm.

The second step is related to the orthogonalization of the principal factors that were retrieved in the first step of FA. This is done in the following section.

2.3.2. Orthogonalization Procedure. The principal spectra retrieved by using the above method are real spectra that are not necessarily independent or mutually exclusive. In other words, these spectra are not spectra of orthogonal factors.[16] Orthogonal factors are not necessary for FA to work. However, real orthogonal factors are necessary to interpret them at the molecular level. Real orthogonal factors generate real abundances and real spectra of pure independent factors. From these, band assignments are unique, and intensities derived from the MFs are exclusive for each factor.[17] Therefore, a second step is necessary to render them orthogonal and the MFs real.

For sugar aqueous solutions, one of the principal factors is pure water. The others are mixtures of pure water and pure hydrates. The procedure for obtaining the orthogonal factors depends on the system. Using only spectral subtractions (I),[18,19] one can produce the needed principal factor spectra. With some practice, the orthogonal factors can be obtained giving, with matrix operations, the MFs (I).[18,20] These are verified to have no negative values.

3. Results and Discussion

3.1. Experimental ATR Spectra. *3.1.1. The Spectra.* The experimental ATR spectra presented in Figures 1 and 2 illustrate the effects of gradually increasing the amount of, respectively, D-glucose and D-fructose in the aqueous solutions. Pure water has a broad intense band from 3000 to 3600 cm^{-1} that contains ν_1 and ν_3; the ν_2 band is at around 1638 cm^{-1}, while near 2115 cm^{-1} is a weak broad combination band. The strong absorption that starts near 1000 cm^{-1} is the libration bands of water, whose

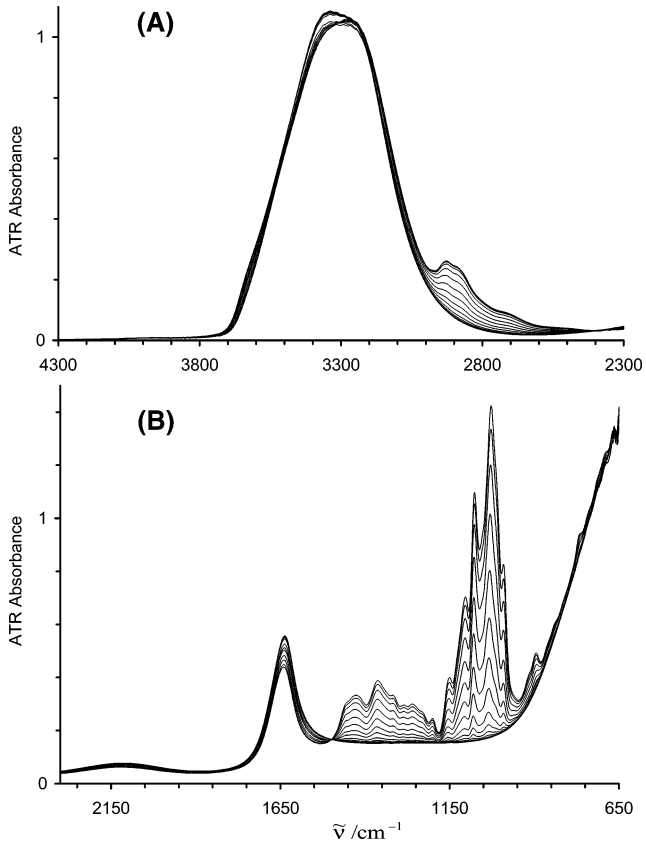

Figure 1. Experimental ATR−IR spectra of 15 mixtures of D-glucose and water. (A) OH and CH stretch regions. (B) Fingerprint and water deformation region.

maximum is around 650 cm^{-1}.[21,22] Figures 1 and 2 show that the water spectrum is not changed much upon carbohydrate addition, although its concentration is greatly decreased (Table 1). This is due to the replacement of the water OH groups by the carbohydrate ones. In the ν_2 region of water (1638 cm^{-1}), where the carbohydrates do not absorb, we observe an intensity decrease due to the diminishing water concentration, although this decrease is tempered by the intensity increase due to the solvated water.

Salient features in both carbohydrate spectra (Figure 1 and 2) are in the 2700−3000 cm^{-1} region of the C−H stretch bands; near 1400 cm^{-1} are low-intensity bands produced by the C−C−H and C−O−H deformation modes, while in the 1000 cm^{-1} region, the intense bands are due to the C−O and C−C stretch vibrations. The spectral signatures of the two carbohydrates are a little different one from another, and they evolve differently. Although the intensity of the CH stretch bands is low, the bands in D-fructose are narrower than those in D-glucose. In the 920 cm^{-1} region, D-glucose shows two small bands assigned to the C−C stretch bands, whereas D-fructose shows only one band with increased intensity. More details are given after the section on FA.

3.1.2. Integrated Intensity of O−H Vibrations in Aqueous Sucrose. Figure 3 shows the molar-integrated intensities of aqueous glucose (a) and fructose (b) as a function of water concentration relative to that of pure water. Frame A displays the molar OH stretch bands (3700−3000 cm^{-1}) normalized to that of pure liquid water.[31] Both curves a and b are nonlinear, although water and glucose or fructose contribute to their intensities, respectively. Frame B displays the molar water deformation band (1750−1500 cm^{-1}) normalized to that of pure liquid water. Although water is the only component that

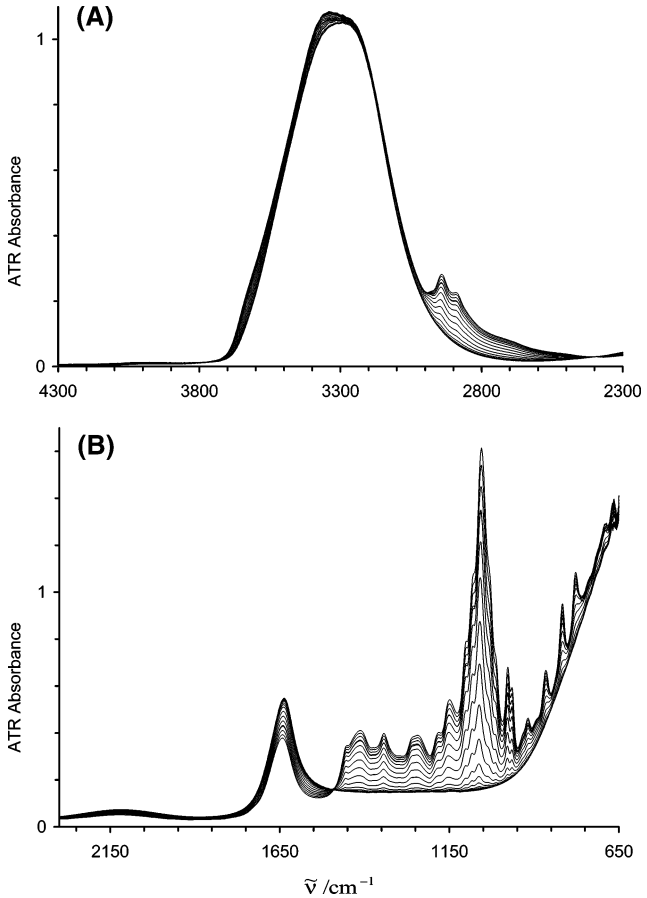

Figure 2. Experimental ATR−IR spectra of 19 mixtures of D-fructose and water. (A) OH and CH stretch regions. (B) Fingerprint and water deformation region.

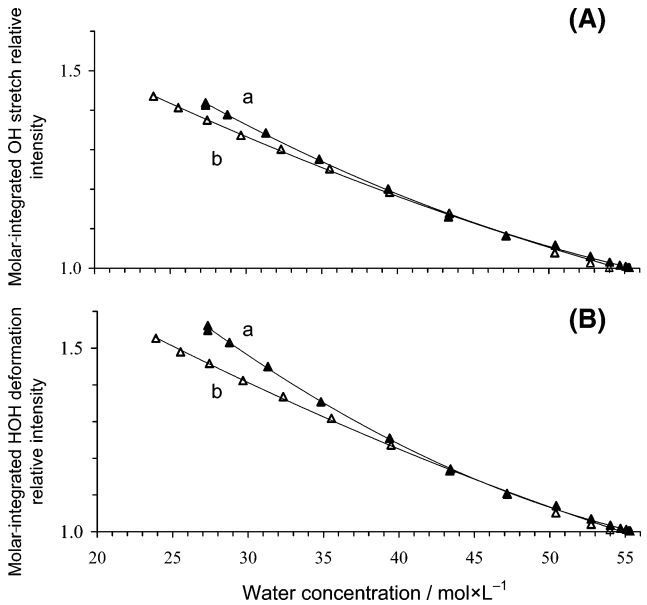

Figure 3. Molar-integrated intensity of (a) D-glucose (full symbol) and (b) D-fructose (empty symbol) aqueous solutions as a function of water concentration relative to pure water measurements. (A) OH stretch band. (B) HOH deformation band.

contributes to this intensity, the curves are nonlinear. Since the integrated intensities of ν_{OH} and δ_{HOH} as a function water concentrations are nonlinear, it indicates that more than two components are present in both carbohydrates solutions. This conclusion is the same as that of aqueous sucrose (I).

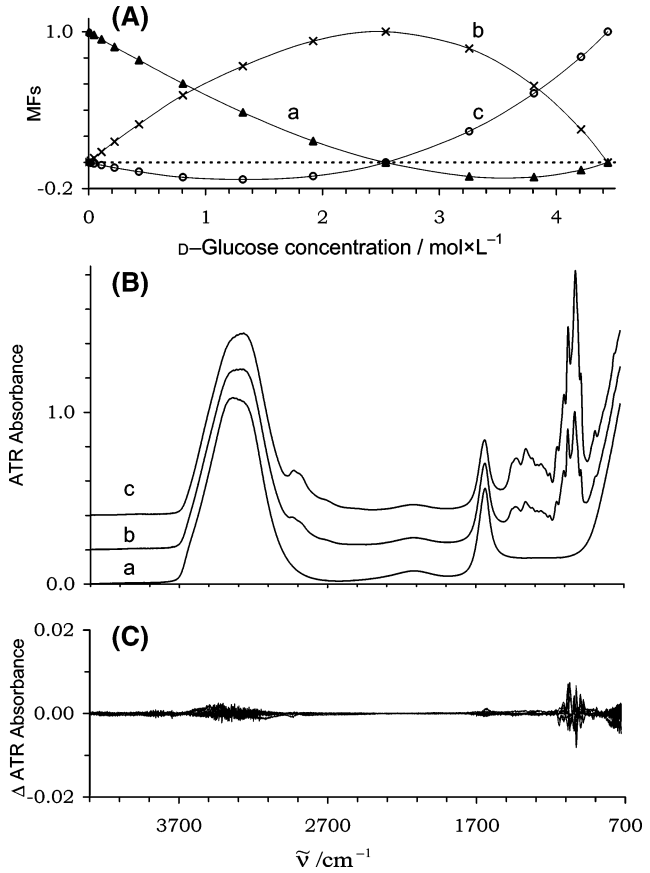

Figure 4. Preorthogonalization FA with three aqueous D-glucose principal factors, (a) pure water, (b) 2.541 M glucose, and (c) 4.440 M glucose. (A) MFs. (B) Experimental spectra. (C) Residues obtained from the difference between calculated ($\sum$ MF × principal spectrum) and experimental spectra of Figure 1.

However, when we look at the handbook data,[23] we find the following relations for the concentrations: [D-glucose] = 8.766 − [H_2O] × 0.1581 and [D-fructose] = 8.822 − [H_2O] × 0.1589. These linear concentration relationships for D-glucose and D-fructose seem to be in contradiction with the integrated intensity measurements. We can push the analysis further by considering that, in aqueous solutions, each sugar molecule takes the place of 6.3 (=1/0.1581, 1/0.1589) water molecules. From the previous relations, we obtain the packing densities by subtracting the water concentrations to give 8.766 and 8.822 mol/L for D-glucose and D-fructose for the densities of 1579 and 1576 g/L, respectively. These values, which are only slightly higher (1.2%) and lower (−1.4%) than that of crystalline D-glucose (D-fructose) at 20 °C,[23] indicate that the packing of both substances is similar to one another and to that of the crystals when water is numerically subtracted. That the relationships of these two isomers are similar would indicate similar interactions with water. The apparent differences between the IR integrated intensities of aqueous glucose and fructose and the above concentration relationships are further analyzed in the following section.

3.2. Factor Analysis Using Three Principal Factors. We first apply FA to the sugar aqueous solutions of glucose and fructose in Figures 1 and 2, respectively, to determine the number of principal factors. For the two sugars, the use of two factors, pure water and one concentrated solution, resulted in systematic nonzero residues. We, therefore, added another one. For glucose (Figure 1), the three principal factors are pure water, the 2.541 spectra, and the 4.440 M spectra. Similarly, in the case of fructose, we used pure water and the 2.560 and 5.009

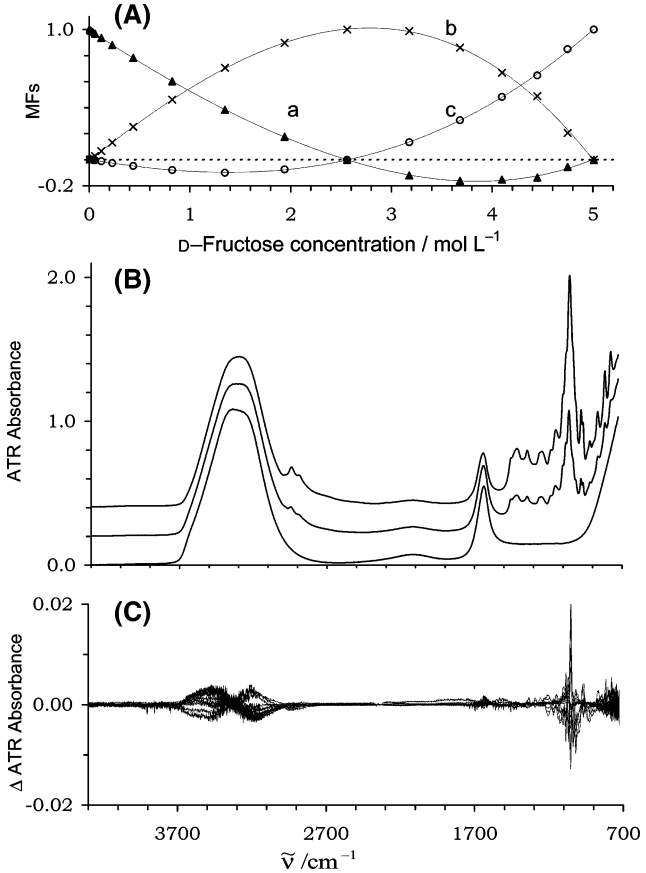

Figure 5. Preorthogonalization FA with three aqueous D-fructose principal factors, (a) pure water, (b) 2.560 M fructose, and (c) 5.009 M fructose. (A) MFs. (B) Experimental spectra. (C) Residues obtained from the difference between calculated ($\sum$ MF $\times$ principal spectrum) and experimental spectra of Figure 2.

M spectra. The principal factors are presented in Figures 4 and 5, respectively. The A frames display the MFs of (a) pure water and (b and c) sugar hydrates spectra. These MFs are associated with abstract factors because parts of the curves are negative. The B frames (Figures 4 and 5) show the principal factor spectra of glucose and fructose, respectively. Although the spectra are real since we used only real spectra, these factors are not orthogonal. Because of this, the MFs are abstract. However, even with nonorthogonal factors, FA can be carried out adequately (I).[24,25] The C frames illustrate the residues obtained from the differences between experimental and calculated spectra. Although low, the residues show some nonrandom signals whose maxima are in the 1000 cm^{-1} region. The maximum level is lower in D-glucose (<0.5% of the most intense band of Figure 1) than in D-fructose (<1.5%). The difference between the two is explained by the narrower and more intense D-fructose band (1.6 AU) than that of D-glucose (1.4 AU) and some temperature variations (I).[21,26] Since these residues are very low, we will not be concerned with them. The overall results indicate that three principal factors are sufficient and necessary to represent the entire sets of aqueous IR spectra of glucose or fructose. This situation is similar to that of aqueous sucrose (I) where three principal factors were obtained, pure water and two hydrates. Since, at this stage, the three principal factors are not orthogonal, we have to render them orthogonal in order to interpret them at the molecular level. This is done below.

3.3. Real MFs and Spectra of the Sugar Hydrates. Given that water and the D-glucose hydrates I and II are the three principal species present in the D-glucose solutions, we can determine their hydration numbers and obtain the real spectra of the orthogonal species through thermodynamic considerations. The first step is to subtract the maximum amount of the water spectrum from both experimental spectra, 2.541 and 4.440 M D-glucose. This is performed keeping in mind that no negative band should appear, especially in the 3700−3650 cm^{-1} region where some OH absorption is present in pure liquid water. After this operation, both hydrate factors are orthogonal to water but not to one another. To render them orthogonal, we push the analysis a step further.

TABLE 2: Principal Factor Matrix before and after Orthogonalization

Matrix	D-Glucose			D-Fructose		
	water			water		
P	1	0	0	1	0	0
	0	1	0	0	1	0
	0	0	1	0	0	1
	water	hydrate I	hydrate II	water	hydrate I	hydrate II
P′	55.341	30.584	15.292	55.309	30.511	14.119
	0	1.2434	1.0682	0	1.5663	1.1735
	0	1.3033	3.3558	0	1.0046	3.8266

3.3.1. Thermodynamic Equilibrium in Aqueous D-Glucose and Hydration Numbers. As for the sucrose hydrates,[4] the D-glucose hydrates contain strongly hydrogen-bonded water. Because the integrated intensity of the aqueous glucose OH bands is not solely related to the species water content (Figure 3), it is not possible to use these bands to determine the hydration numbers. Therefore, to obtain the hydrate composition of aqueous glucose, we will use the method that worked for sucrose (I). We set up a chemical equilibrium between the two hydrates by assuming that the two D-glucose hydrates contain *m* and *n* water molecules, respectively. It is well-known that liquid water molecules form strong H bonds with neighboring molecules and form strong bonds with the carbohydrate molecules. We will use a pair of molecules to represent liquid water. Therefore, the transfer of one water molecule from the bulk to form a glucose hydrate can be done by breaking at least one H bond of a pure water pair. Thus, the equilibrium equation and its constant are

$$(m-n)\,(H_2O)_2 + 2(C_6H_{12}O_6{\cdot}nH_2O) \rightleftarrows 2(C_6H_{12}O_6{\cdot}mH_2O) \quad (4)$$

$$K_G = \frac{[C_6H_{12}O_6{\cdot}mH_2O]^2}{[C_6H_{12}O_6{\cdot}nH_2O]^2[(H_2O)_2]^{m-n}} \quad (5)$$

The principal factor matrix **P** used for the determination of the number of principal factors is a unit matrix (Table 2). We reported that the principal factor matrix **P** (that contains the sample compositions) can be modified into another one that we call **P′** that modifies **MF** to yield **MF′**, which are obtained by matrix multiplication (I).[18]

$$\mathbf{MF'} = \mathbf{P'} \times \mathbf{P}^{-1} \times \mathbf{MF} \quad (6)$$

Equation 6 is subject to the following condition; the same subset of experimental spectra ($\mathbf{S}^{\mathbf{P}}_{\mathrm{exp}}$) is selected to calculate the principal factor spectra. Equation 6 gives the calculation matrix method used. Matrices **MF** and **P** are known from previous calculations; matrix **P′** is determined (adjusted), while **MF′** is calculated simply using eq 6.[32] The new **MF′** obtained through eq 6 ensures that the residues obtained are identical to those obtained using **MF** and **P** (I).[18] With eqs 5 and 6 at hand and

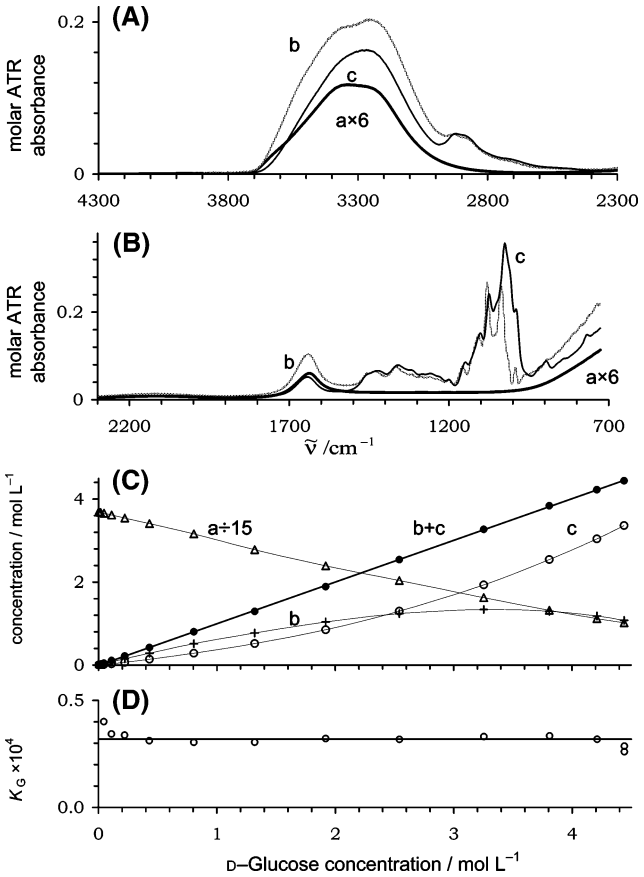

Figure 6. FA with three aqueous D-glucose principal factors (after orthogonalization), (a) pure water, (b) D-glucose pentahydrate, and (c) dihydrate. (A) and (B) Spectra. (C) Species concentration. (D) Equilibrium constant, K_G.

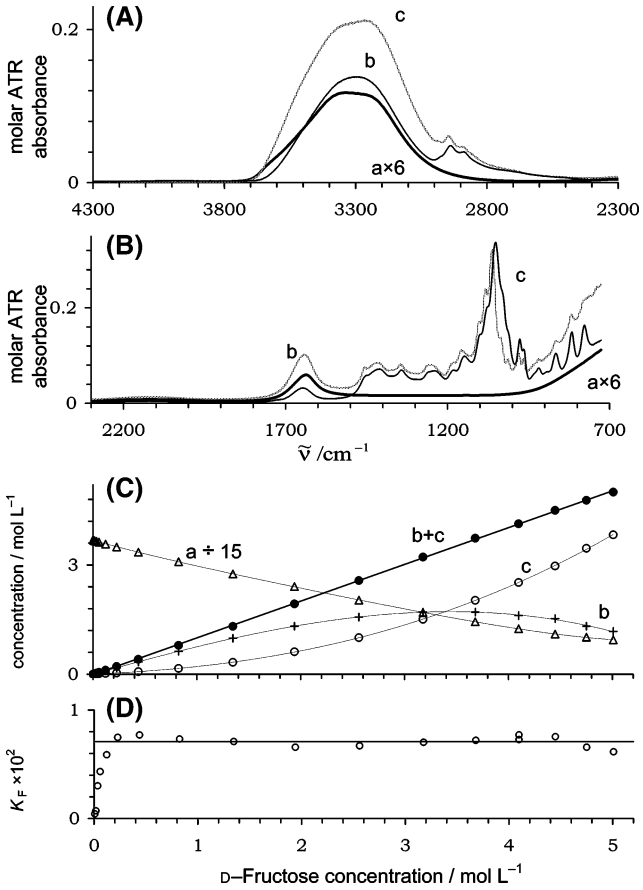

Figure 7. FA with three aqueous D-fructose principal factors (after orthogonalization), (a) pure water, (b) D-fructose pentahydrate, and (c) dihydrate. (A) and B) Spectra. (C) Species concentration. (D) Equilibrium constant, K_F.

looking at the principal factor spectra (taking care that no negative band appears), matrix **P′** is modified until a constant value of the calculated equilibrium constant K_G is obtained for the entire solution range. This is made by trial and error with different sets of (m, n) until a set is obtained that maintains the experimental value of K_G almost constant. For aqueous solutions of D-glucose, we obtained the set $m = 5$ and $n = 2$. Matrix **P′** is obtained from Table 2. It represents the matrix of the principal species's concentrations in the experimental solutions used to form the principal factor analysis. The factors obtained are illustrated in Figure 6. Frames A and B show the orthogonal factor spectra: (a) pure water, 1 M, (b) D-glucose pentahydrate, 1 M, and (c) D-glucose dihydrate, 1 M. Frame C shows the real species concentration. The residues are identical to those presented in Figure 4C. Finally, frame D shows the equilibrium constant K_G at $(3.2 \pm 0.6) \times 10^{-5}$ L^3 mol^{-3} in the range of 0.1−4.5 M D-glucose. Below this range, the uncertainty is too large to give reliable values. The value of the constant is close to that of aqueous sucrose ($K_e = (4.1 \pm 0.3) \times 10^{-5}$ L^3 mol^{-3}), for which two similar hydrates were observed, sucrose penta- and dihydrates (I).

Looking at the abundance curves as a function of glucose concentration (Figure 6C), that of pure water is a maximum at the zero glucose level and decreases as the glucose concentration increases. Following the same concentration gradient, glucose pentahydrate (curve b) starts at the zero level and reaches a plateau at 3.2 M glucose, whereupon it decreases. Glucose dihydrate (curve c) starts at the zero level, increases slowly following a second-order curve, crosses the pentahydrate curve at ∼2.5 M glucose, and continues up to the maximum concentration. It is informative to note that the sum of the penta- and monohydrate concentrations as a function of total prepared glucose concentration gives a linear curve (b + c = 1.0034x − 0.0056), whereas those of the individual hydrates are not.

3.3.2. Thermodynamic Equilibrium in Aqueous D-Fructose and Hydration Numbers. The same procedure was applied to fructose hydrates, giving the values of $m = 5$ and $n = 1$ for the constant set, indicating that the fructose aqueous solutions are composed of pure water and penta- and monohydrates. Matrix **P′** and the real species concentrations are given in Table 2. The equilibrium equation for fructose and its equilibrium constant are

$$2(H_2O)_2 + C_6H_{12}O_6{\cdot}H_2O \rightleftarrows C_6H_{12}O_6{\cdot}5H_2O \qquad (7)$$

$$K_F = \frac{[C_6H_{12}O_6{\cdot}5H_2O]}{[C_6H_{12}O_6{\cdot}H_2O][(H_2O)_2]^2} \qquad (8)$$

The results are illustrated in Figure 7. Frames A and B display the orthogonal factor spectra, (a) pure water, 1 M, (b) and (c) D-fructose pentahydrate and monohydrate, 1 M, respectively. Frame C displays the species concentration. Finally, frame D shows the equilibrium constant, which is constant at $K_F = (7.1 \pm 1.2) \times 10^{-3}$ L^2 mol^{-2} in the range of 0.11−5.00 M. This constant is not significantly different from that of glucose (3.2×10^{-5} L^3 mol^{-3}).[33] Although the fructose hydrate concentrations are very similar to those of glucose (Figures 7C and 6C, respectively), we note that the maximum concentration of fructose pentahydrate is 1.6 M (ordinate scale) near the 3.2 M (abscissa scale) total fructose concentration, whereas that of

TABLE 3: Comparison of the Band Molar-Integrated Intensities of the Five Carbohydrate Hydrates with that of Water

Species	D-Glucose			D-Fructose		Sucrose [a]	
	pure H_2O	pentahydrate	dihydrate	pentahydrate	monohydrate	pentahydrate	dihydrate
integrated OH stretch molar absorption[b] in AU × cm^{-1} × L/mol	8.30	92.55	66.97	93.41	54.06	145.07	101.12
number of OH groups	2	15	9	15	7	18	12
total OH stretch molar absorption[b] in AU × cm^{-1} × L/mol (OH)	4.15	6.09	7.53	6.23	7.72	8.06	8.43
relative to pure water	1.00	1.47	1.81	1.50	1.86	1.92	2.01
integrated water ν_2 molar absorption in AU × cm^{-1} × L/mol	1.12	2.24	2.83	2.19	3.13	3.40	3.95
relative to pure water	1.00	2.00	2.53	1.95	2.80	2.88	3.35

[a] Ref 4. Since the path length for the sucrose study was different from that used for this one, the sucrose values were renormalized using water as a standard to have comparable situations. [b] Integrated molar intensity of the OH stretch band divided by the OH concentrations: I_{OH}/[OH].

glucose is 1.2 M at 3.0 M, respectively. The differences in the hydrate concentrations and the equilibrium constants are due to the presence of the monohydrate in the case of fructose solutions and a the dihydrate in the case of D-glucose. Here again, we note that the sum of the penta- and monohydrate concentrations as a function of total prepared glucose concentration gives a linear curve ($b + c = 1.0091x - 0.0127$), whereas those of fructose penta- and monohydrates are nonlinear.

3.3.3. Comments on the Thermodynamic Equilibrium of the Species in Aqueous Glucose and Fructose. For aqueous solutions of glucose and fructose, as for sucrose previously (I), we find that three species are present in the solutions, pure water, pentahydrates, and dihydrates for glucose and sucrose and pure water, pentahydrate, and monohydrate for fructose. After transforming the nonorthogonal factors into orthogonal ones, neither the water factor nor the hydrate factors were linear as a function of the prepared solutions. It is only after adding the two hydrates for glucose and fructose that we obtain linear relationships as a function of the prepared concentrations.

3.4. Spectral Features of Aqueous Glucose and Fructose Hydrates. *3.4.1. Comparison between Aqueous Glucose Pentahydrate and Dihydrate.* The spectra of pure glucose pentahydrate and dihydrate (both normalized to 1 M) are shown in Figure 6A and B along with the spectrum of pure water. Second derivatives were used to obtain the band positions whose assignments are made in Table 4. Both hydrate spectra are similar, having bands at almost the same places with mostly comparable intensities. In most of the spectral region (5500−700 cm^{-1}), the species' spectra are not much different from one another except for small intensity variations. However, the ethoxy region (1200−900 cm^{-1}) is the notable exception because the numerous bands in this region are a little displaced with many intensity variations. Each species has some particularities that enabled us to separate them. Furthermore, this region is free of water, making these spectra the characteristic signatures of the species. This is a clear advantage of FA that permitted the separation of the hydrate species in the sugar aqueous solutions.

As expected, the biggest differences in the spectra of the glucose solution species involve the OH groups (Figure 6A). The ν_{OH} band near 3300 cm^{-1} is assigned to the OH stretch vibrations of water (ν_1, ν_3, and their satellites) and those of glucose. The ν_1 and ν_3 bands (Table 4) are situated at 3389 and 3222 cm^{-1} in pure liquid water.[21] The manifestation of these two bands is clearly displayed in Figure 6A by the nearly flat top of the absorption. These bands are displaced with an intensity ratio modification to 3385 and 3212 cm^{-1} in the pentahydrate and to 3380 and 3225 cm^{-1} in the dihydrate, respectively. It was impossible to separate the ν_{OH} band of carbohydrate from the water ν_1 band. The intensity of these hydrate massive bands is assigned to both water OH and glucose OH vibrations. However, taking into account the relative intensity of the two OH stretch bands of water, it is possible to estimate that the glucose OH band position is close to that of the ν_1 of water. In pure water, the two bands have similar intensities producing the flat top of the absorbance (Figure 6A trace a). In glucose pentahydrate, the blue band intensity is lower than the intensity of the red one so that the former is a clear shoulder (Figure 6A trace b). In glucose dihydrate, the intensity of the ν_3 band of water is far lower than the combined one of the ν_1 band of water and the ν_{OH} band of glucose. Therefore, the blue shoulder is still observed in Figure 6A trace c but needs the use of the second derivative in order to be identified. A similar situation was observed in acetone methanol mixtures; following the same pattern under the different H−bonding situations, the uncoupled OH vibration of methanol was found to be close to ν_1 of water.[19]

In the CH stretch region (~2900 cm^{-1}, Figure 6A), the two principal CH bands are blue shifted from penta- to dihydrate by 4 cm^{-1} with not much intensity variation. These small differences indicate that the glucose CH groups are very similar in the two hydrates.

The HOH deformation band (Figure 6B) goes from 1638 to 1640 and to 1642 cm^{-1} from the pure water situation to the pentahydrate and to the dihydrate, respectively. This band shows a nonlinear intensity increase along with increasing glucose concentration (decreasing water concentration, Figure 3B), although this band is entirely due to water. This indicates that the water deformation band is modified when pure water is transformed into the hydrated forms. The H−C−H and H−O−C deformation bands in the 1500−1200 cm^{-1} region (Figure 6B) show only a small intensity difference. This indicates that these groups are only very slightly modified in passing from penta- to dihydrate.

In the C−O stretch region (1000 cm^{-1}, Figure 6B), we observe the major differences between the two glucose hydrates. However, the band positions in this region are not much different from one hydrate to the other (Table 4); the pentahydrate bands at 1081 and 1034 cm^{-1} are displaced to 1076 and 1027 cm^{-1} in the dihydrate, respectively. These small displacements are accompanied by important intensity variations. The intensity of the red band increases, while that of the blue one decreases. Such a red shift of the C−O stretch bands could be related to an increase of the strength (or the number) of the H bond(s)

TABLE 4: Band Positions (in cm^{-1}) of Aqueous Sucrose, D-Glucose, and D-Fructose

	Kodad et al.[29]		Max et al.[4]		Max et al.[21]	This Work			
assignment[a]	solid sucrose	aqueous sucrose	sucrose $(H_2O)_5$	sucrose $(H_2O)_2$	H_2O	glucose $(H_2O)_5$	glucose $(H_2O)_2$	fructose $(H_2O)_5$	fructose (H_2O)
					~5200	~5187		~5180	
					3630	~3612			
						3530	3505	3520	~3510
ν_3 H_2O + νOH			~3350	~3290	3389[b]	3385	3380	3385	3369
ν_1 H_2O + νOH			~3240	~3240	3222[b]	3212	3225 d	3225	3236
νCH_3 as			2974	2970				2986	2981
νCH_2 as			2938	2933		2925	2930	2946	2940
νCH_2 s			2882	2880		2870	2885	2887	2884
comb.			2850	2843			2860	~2855	
comb.			2680	2680					
comb.			~2500	~2500					−2505
ν_2 H_2O + $\nu_L H_2O$			~2125	~2125	2115	~2120	2130	2125	2122
ν_2 H_2O		1640	1645	1648	1638	1640	1642	1645	1648
	1461								
		1451	1454	1452			1462	1458	1457
δC−O−H[c]	1431	1430	1425	1420		1435 w	1420	1429	~1425
	1410							1410	1407
δC−O−H glu[c]	1370	1366	1370	1370		1368	1362	1375	1374
δC−O−H fru[c]	1346	1336	1333	1331			1335	1344	1342
	1323					1316	1315	1318	
	1280					1288	1284	1299	1294
δCH_2[c]		1265	1275	1270		1263	1260	1264	1262
ωCH_2[c]	1239	1247				1230	1226	1243	1236
			1210	1210		1201	1199	1218	
								1187	1185
	1162					1158	1151	1158	1152
νCO endo fru[c]	1130	1136	1135	1132		1132 sh			
νC−O endo glu[c]	1106	1113	1113	1110		1106 sh	1102	1104 m	1102 m
	1069					1081 s	1076 m	1084 m	1080 m
νC−O	1052	1055	1055 vs	1045 vs		1058	1053 sh	1062 s	1053 s
						1034 s	1027 m	1033 sh	1028 sh
δC−O−H	1008					1013	1008 sh	1014 sh	1010 sh
νC−O exo	990	993	998 vs	993 vs		991.5	988	993	~994
								980 m	978 m
								966 m	963 m
νC−C glu[c]	941	945				936		936	936
							919	919	918
νC−C fru[c]	911	925	929	928		895	895	~891	895
νC−C[c]	867	870	868	868		863	863	868 m, d	866 m, d
	849								
δC_2-C_1-H glu[c]		835				837	841	838	839
δC_3-C_2-H fru[c]		828		830				820 m	817 m
									797
							769		778 m
									~740

[a] The water bands are identified by H_2O; the other bands are those of sucrose. [b] Obtained by Gaussian band fitting. [c] The assignments made by Kodad et al.[29] Abbreviations: fru, D-fructosyl moiety; glu, D-glucosyl moiety; δ, deformation; ν, stretch; τ, torsion; ω, wag; endo, endocyclic; exo, exocyclic; s, strong; d, double; m, medium; sh, shoulder; w, weak.

accepted by the oxygen atom involved in the bond that modifies the dipole moment responsible for the band intensities.[18,19]

Some differences between penta- and dihydrates are observed in the CC stretch region (~900 cm^{-1}, Figure 6B) where the two hydrates have weak bands with different positions and intensities. Below this region, we note some small intensity differences, mainly due to the difference in water content of the two species since the far wing of the water libration bands (ν_{max} at 613 cm^{-1})[22] starts to absorb near 1100 cm^{-1}. The two species are affected differently by this absorption. However, it is the variation of the 991.5 and 936 cm^{-1} band intensities that allowed us to separate the spectra of the two glucose species.

3.4.2. Comparison between Aqueous Fructose Pentahydrate and Monohydrate. The spectra of pure fructose pentahydrate and monohydrate (both normalized to 1 M) are shown in Figure 7A and B along with that of pure water. Second derivatives were used to obtain the band positions whose assignments are made in Table 4. The features of fructose penta- and monohydrates in water are very similar to those of glucose with small differences. The CH stretch bands of fructose pentahydrate are at higher frequencies (2946 and 2887 cm^{-1}) than those of glucose (2925 and 2870 cm^{-1}). The CH stretch bands of fructose pentahydrate are slightly red shifted when it is transformed into dihydrate, whereas they are blue shifted in the case of glucose (Table 4).

The strongest fructose band modifications arise in the 1000 cm^{-1} region (Figure 7B). The 1062 cm^{-1} band of the pentahydrate shifts to 1053 cm^{-1} in the monohydrate accompanied by intensity variations. Similar variations were observed in the penta- to dihydrate shifts with sucrose and glucose. However, the principal differences between the sugars in this region are the presence of a single strong band in the fructose spectra, whereas two bands are present in the glucose (Figure 6B) and sucrose (I) spectra.

3.4.3. Water Deformation Band in Aqueous Glucose and Fructose. The 1640 cm^{-1} region that contains no sugar

absorption contains the water HOH deformation (δ_{HOH}) band. Upon the formation of the glucose fructose hydrates, this band is slightly blue shifted (Figures 1 and 2) as with sucrose (I). The molar-integrated intensity increases by more than a factor of 2 (Figure 3B and Table 3). A similar result was obtained with sucrose (I). Since only water absorbs in this region, the formation of the hydrates causes a modification of the dipole moments responsible for the intensity increase. Three factors can influence this water band intensity of the sugar hydrates. The first one is the refractive index of the absorbing components. In previous papers, we have shown that the ATR absorption of solvated water is affected by the fourth power of the refractive index.[20,25] For example, in aqueous 5.22 M fructose aqueous solutions (high concentration), the refractive index is 1.45.[23] Compared to water (1.33), the variation is about 9%.[23] The second factor is the density variation that increases the absorption slightly. The third factor is the absorptivity of the chromophores. Since the first two factors contribute minimally to the band intensity increase, most of the increase comes from the third factor. This increase can be rationalized by the following scheme. When water forms a hydrate, it must adapt its shape to accommodate the available sites to form H bonds with the sugar host. This accommodation produces a dihedral angle decrease that results in a dipole moment increase, which in turn, contributes to the intensity increase. Recall that the water deformation (δ_{HOH}) band is due to the variation in the HOH dihedral angle. Such an increase has previously been observed in aqueous acetonitrile.[27]

3.4.4. Integrated Intensities of the OH Stretch in Aqueous Glucose and Fructose. Although the OH stretch region shows an intensity increase by a factor of 1.5 and more, it is difficult to separate the contribution of carbohydrates from that of the hydrates. All of the OH groups, either from the carbohydrates or from water, form H bonds since we observe no free OH groups. On the carbohydrates, the H on the OH groups can make one H bond, and the oxygen of these groups can receive up to two H bonds, while the acetal oxygen can receive two H bonds. Therefore, H-bond acceptors are in large excess in aqueous carbohydrate solutions. This explains why no "free" OH vibration could be found. This situation gives 17, 17, and 30 H-bond sites for glucose, fructose, and sucrose, respectively. Since water can make two H bonds and receive two H bonds, this gives 20 H bonds for the pentahydrates. For glucose and fructose, the surplus H bonds could be shared with other groups intramolecularly or intermolecularly. For sucrose, there is a surplus of sites not filled with water. This is an indication of an overlapping of the two moieties favoring intramolecular H bonds that obstruct the sites for inserting water.

As for the water deformation band, the intensity of the OH stretch band also shows an increase upon solvation with the sugars. However, this increase comes from the solvated water and the OH groups of the sugars. We try to evaluate it by comparing it to the integrated intensity of water since it is the yardstick. The molar-integrated intensity of the OH stretch band measured from the water IR spectrum (Figure 7A) is 8.30 AU $\times$ cm^{-1} $\times$ L/mol, which, for one OH group, is 4.15 AU $\times$ cm^{-1} $\times$ L/mol (Table 3). For the solvated sugar, the mean value for the glucose and fructose pentahydrates is 6.16 $\pm$ 0.10 AU/cm mol^{-1} of OH groups, and that of the dihydrate glucose and monohydrate fructose is 7.62 $\pm$ 0.13 AU/cm mol^{-1} of OH groups. Compared to the intensity of the water OH group, the sugar hydrates show an increase by a mean factor of 1.73 (Table 3). This factor is lower than that observed for the solvated water deformation band, but the OH stretch band contains many

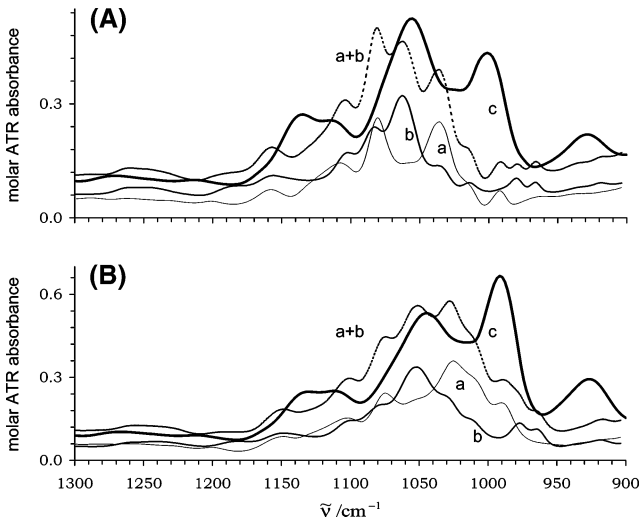

Figure 8. Comparison between the different IR molar spectra of sugar aqueous hydrates in the C−O and C−C stretch regions. (A) Pentahydrates of (a) D-glucose, (b) D-fructose, and (c) sucrose. (B) Dihydrate of (a) glucose and (c) sucrose and (b) fructose monohydrate.

elements that contribute differently to its intensity, ν_3 and ν_1 of solvated water and ν_{OH} of the carbohydrates. A similar increase was observed for the OH absorption of aqueous propanol.[28]

The same three factors that influence the water deformation band influence, as well, the OH stretch band intensity of the sugar hydrates. Here, the refractive index and density variations contribute but a small part of the band intensity increase. Most of the increase must come from the increased absortivity of the solvated sugar chromophores, which is higher than that of pure water. Such a situation has already been reported for propanol and methanol,[19,28] and had been deduced for sucrose (I). For methanol[19] and solvated sucrose (Table 3), the OH absorption is nearly twice that of water. The OH of pure water produces two vibrations with no bulk group to enhance their movements. The methanol and the sugars' OH groups have only one stretch vibration per OH group. Furthermore, the oxygen atoms are attached to a bulk group. These situations would amplify the vibration amplitude and, consequently, the dipole moment responsible for the band intensity. These different contexts explain the intensity variation observed for water and alcoholic molecules (methanol and sucrose hydrates). The slightly lower values observed for glucose and fructose hydrates (Table 3) are explained in the following way: (1) these sugars have three OH groups less than that of sucrose and (2) the solvated water molecules are perturbed (as we have seen for the deformation band) but not as much as the alcoholic OH. At this stage, it is difficult to separate the contribution of carbohydrate OHs from those of the solvated water. The use of heavy water to substitute the water hydrogen atoms by deuterium will also substitute those of the carbohydrate. This mixture will give a cocktail of species that cannot be easily separated.[21] The problem of determining the absorptivity of the carbohydrate OH groups is still an open one, although we can indicate that they are higher than that of pure water.

3.5. Comparison between the IR Molar Spectra of the Carbohydrates' Hydrates. Figure 8 illustrates the ethoxy region (1200 to 900 cm^{-1}) of the hydrates of glucose (from Figure 6B), fructose (from Figure 7B), and sucrose (from I). To these, we have added the sum of the glucose hydrates to the corresponding hydrates of fructose that can be compared with those of sucrose. All of the spectra are on the molar basis. However, the glucose (trace a) and fructose (trace b) molecules have 7 C−O groups, whereas that of sucrose (trace c) has 14.

The number of C−O groups is directly linked to the intensities; that of sucrose is approximately twice that of the glucose and fructose traces. Table 4 gives a tentative assignment of the bands based on a solid and aqueous sucrose study.[29] A normal coordinate analysis of these systems, which is in progress, should verify and refine these assignments. Nonetheless, we can follow the principal bands going from glucose to fructose and to sucrose.

3.5.1. Pentahydrates of Sucrose, Glucose, and Fructose. Figure 8A illustrates the spectra of pentahydrates of sucrose, glucose, and fructose. The glucose spectrum (trace a) shows two medium intensity bands at 1081 and 1034 cm^{-1}. In fructose (trace b), these bands merge into one main band situated midway at 1062 cm^{-1} and a smaller component at 1084 cm^{-1}. The sum of these spectra gives rise to trace a + b. The sucrose spectrum (trace c) has an intensity comparable to that of trace a + b, reflecting that sucrose is composed of glucose and fructose moieties. However, the bands have shifted. This reflects a conformation change and the transformation of one OH group on each moiety into the new acetal C−O−C group, which absorbs in the 1000 cm^{-1} range since there is little absorption at this position in the monosaccharides. In sucrose pentahydrate (Figure 8A trace c), the C−C stretch band appears as a well-defined band near 930 cm^{-1}, whereas those of the monosaccharides are at higher frequencies with little intensity. Here again, these modifications reflect the conformational differences in the sugars.

3.5.2. Dihydrates of Sucrose and Glucose and the Monohydrate of Fructose. Figure 8B illustrates the spectra of the dihydrates of sucrose and glucose and the monohydrate of fructose. The glucose spectrum (trace a) shows one bulky medium-intensity band at 1027 cm^{-1} with satellite components. This absorption pattern indicates a conformational change of the dihydrate compared to that of the pentahydrate. In fructose (trace b), these bands are displaced to higher frequencies and are almost unchanged, where the most intensive band is now situated at 1053 cm^{-1}. This position is a little lower than that of the pentahydrate (1062 cm^{-1}), but the overall pattern is not changed much. This indicates that the conformation is little changed in passing from the penta- to the monohydrate. This is different than in glucose and indicates that fructose, a five-atom cycle, is more rigid than glucose, a six-atom one. The sum of the two spectra gives trace a + b whose intensity can be compared to that of trace c, the sucrose dihydrate spectrum. As in the pentahydrates, the integrated intensity of the two traces is similar, but the bands have shifted in the sucrose spectrum. The two main bands of the monosaccharides at 1053 and 1027 cm^{-1} have coalesced into the 1045 cm^{-1} band, and a new band at 993 cm^{-1} has emerged. This band that we assign to the acetal is almost at the same place as in the sucrose pentahydrate (991.5 cm^{-1}). However, the acetal band in the sucrose dihydrate (Figure 8Bc) is a little more intense and narrower than in the pentahydrate (Figure 8Ac), reflecting a difference in the strain of this bonding. In sucrose dihydrate (Figure 8Bc), the C−C stretch band appears as a well-defined band near 928 cm^{-1}. This band is almost at the same position but is more intense than that of the pentahydrate, reflecting differences in the conformational organizations.

4. Conclusion

The infrared study, via the ATR setup, of aqueous solutions of glucose and fructose in the concentration range from pure water to the saturation limit revealed that the solutions are composed of pure water and two hydrates. For these, we obtained the real spectra of the orthogonal factors and their abundances as a function of the sugar concentrations. Except for pure water, the two hydrates are present in the whole solubility range. For D-glucose, the species are the pentahydrate ($C_6H_{12}O_6 \cdot 5\ H_2O$), more abundant in the lower solubility range, and the dihydrate ($C_6H_{12}O_6 \cdot 2\ H_2O$), more abundant in the higher solubility range. Although the literature refers repeatedly to the existence of glucose monohydrate, we found no evidence of it, although this possibility cannot be ruled out entirely because it could exist at the saturation limit. The equilibrium constant between the two hydrates is $K_G = 3.2 \times 10^{-5}\ L^3\ mol^{-3}$. These results are similar to the penta- and dihydrates that we obtained for sucrose (I) with the equilibrium constant $K_e = 4.1 \times 10^{-5}\ L^3\ mol^{-3}$. For D-fructose, the species are the pentahydrate ($C_6H_{12}O_6 \cdot 5\ H_2O$), more abundant in the lower solubility range, and the monohydrate ($C_6H_{12}O_6 \cdot H_2O$), more abundant in the higher solubility range. We found no evidence of a dihydrate. The equilibrium constant between the two hydrates is $K_F = 7.1 \times 10^{-3}\ L^2\ mol^{-2}$. Although the two glucose and fructose hydrates retrieved do not present linear abundances as a function of the prepared concentrations, the sum of their concentrations is linear. The linear relationship of the species retrieved by IR spectroscopy is valid in the complete solubility range of D-glucose and D-fructose, whereas the use of only one carbohydrate species gives a linear relationship only in a limited concentration range.

For glucose and sucrose dihydrates, the two water molecules cannot occupy all of the available sites of the sugars. That all of the OH groups of the carbohydrates and water form H bonds indicates that intramolecular bonding is present: split H bonds of water to adjoining acceptor groups on the sugars, the formation of sugar dimers, or any combination of these. However, although dimer formation is a possibility, we found no evidence of band splitting that would suggest so. The other possibilities can be obtained through conformational optimization that favors intramolecular H bonding when intra- and intermolecular bonding is possible. For fructose monohydrate, the ring is more rigid than that of glucose and consequently has less mobility to change its organization to accommodate H−bonded water. This explains the formation of the monohydrate instead of the dihydrate.

Appendix

Multiplying Factors (MFs) from the Spectra Scalar Products. Multiplying each term of eq 1 by the transpose of the principal factor spectra matrix $(\mathbf{S^P})^T_{f,l}$ gives

$$(\mathbf{S^P})^T_{f,l} \times (\mathbf{S^e})_{l,n} = (\mathbf{S^P})^T_{f,l} \times (\mathbf{S^P})_{l,f} \times (\mathbf{MF})_{f,n} + (\mathbf{S^P})^T_{f,l} \times (\mathbf{R^e})_{l,n} \quad \text{(A1)}$$

Multiplying the terms of this equation by the inverse matrix of the scalar products of the principal factor spectra $[(\mathbf{S^P})^T_{f,l} \times (\mathbf{S^P})_{l,f}]^{-1}{}_{f,f}$ yields

$$[(\mathbf{S^P})^T_{f,l} \times (\mathbf{S^P})_{l,f}]^{-1} \times (\mathbf{S^P})^T_{f,l} \times (\mathbf{S^e})_{l,n} = (\mathbf{MF})_{f,n} + [(\mathbf{S^P})^T_{f,l} \times (\mathbf{S^P})_{l,f}]^{-1} \times (\mathbf{S^P})^T_{f,l} \times (\mathbf{R^e})_{l,n} \quad \text{(A2)}$$

From eq A2, we obtain the multiplying factor matrix $(\mathbf{MF})_{f,n}$

$$(\mathbf{MF})_{f,n} = [(\mathbf{S^P})^T_{f,l} \times (\mathbf{S^P})_{l,f}]^{-1} \times (\mathbf{S^P})^T_{f,l} \times (\mathbf{S^e})_{l,n} - [(\mathbf{S^P})^T_{f,l} \times (\mathbf{S^P})_{l,f}]^{-1} \times (\mathbf{S^P})^T_{f,l} \times (\mathbf{R^e})_{l,n} \quad \text{(A3)}$$

In eq A3, there are three scalar product matrices, (i) the scalar products of the principal factor spectra with themselves, $[(\mathbf{S^P})^{\mathrm{T}}_{f,l} \times (\mathbf{S^P})_{l,f}]_{f,f}$; (ii) the scalar products of the principal factor spectra with each of the experimental spectra, $[(\mathbf{S^P})^{\mathrm{T}}_{f,l} \times (\mathbf{S^e})_{l,n}]_{f,n}$; and (iii) the scalar products of the principal factor spectra with all of the residue spectra, $[(\mathbf{S^P})^{\mathrm{T}}_{f,l} \times (\mathbf{R^e})_{l,n}]_{f,n}$.

The minimum number of principal factors is obtained when the right-most term in eq A3 is close to the null matrix. With this number at hand, eq A3 gives the MFs of the principal factor spectra $(\mathbf{S^P})_{l,f}$. The residues $(\mathbf{R^e})_{l,n}$ give the MFs accuracy; a low level indicates a high accuracy. This means that the difference between the recombined spectra and the original spectra must be zero, within experimental error. To this end, a very low value must be obtained for the scalar products between each of the principal factor spectra and each of the residue spectra

$$(\mathbf{S^P})^{\mathrm{T}}_{f,l} \times (\mathbf{R^e})_{l,n} \cong 0 \qquad \text{(A4)}$$

References and Notes

(1) Scatchard, G. *J. Am. Chem. Soc.* **1921**, *43*, 2406.
(2) Sugden, J. N. *J. Chem. Soc.* **1926**, *129*, 174.
(3) Immel, S.; Lichtenthaler, F. W. *Liebigs Ann.* **1995**, *11*, 1925.
(4) Max, J.-J.; Chapados, C. *J. Phys. Chem. A* **2001**, *105*, 10681.
(5) Lendl, B.; Kellner, R. *Mikrochim. Acta* **1995**, *119*, 73.
(6) Cadet, F.; Robert, C.; Offman, B. *Appl. Spectrosc.* **1997**, *51*, 369.
(7) Kameoka, T.; Okuda, T.; Hashimoto, A.; Noro, A.; Shiinoki, Y.; Ito, K. *J. Jpn. Soc. Food Sci. Technol.* **1998**, *45*, 199.
(8) Hashimoto, A.; Kameoka, T. *Appl. Spectrosc.* **2000**, *54*, 1005.
(9) Hashimoto, A.; Nakanishi, K.; Motonaga, Y.; Kameoka, T. *Biotechnol. Prog.* **2001**, *17*, 560.
(10) Because of the high water absorbtivity, a cell with a reduced path length was made. The effective number of reflections was determined with the pure water spectrum of Bertie, J. E.; Lan, Z. *Appl. Spectrosc.* **1996**, *50*, 1047.
(11) Wieliczka, D. M.; Weng, S.; Querry, M. R. *Appl. Opt.* **1989**, *28*, 1714.
(12) Savitzky, A.; Golay, M. J. E. *Anal. Chem.* **1964**, *36*, 1627.
(13) Malinowski, E. R.; Howery, D. G. *Factor Analysis in Chemistry*; Robert E Krieger Publishing Co.: Malabar, FL, 1989.
(14) Chapados, C.; Trudel, M. *Biophys. Chem.* **1993**, *47*, 267.
(15) Brereton, R. G. *Multivariate Pattern Recognition in Chemometrics*; Elsevier: Amsterdam, The Netherlands, 1992.
(16) The expression "orthogonal spectra" cannot be used because the integrated product of two real spectra is not zero.
(17) The factors are the terms obtained from FA. The species, which are the physical entities, may be the same or a multiple of these factors, depending on the evolving nature of the species.
(18) (a) Max, J.-J.; Chapados, C. *J. Chem. Phys*. **2003**, *119*, 5632. (b) Max, J.-J.; Chapados, C. *J. Chem. Phys*. **2004**, *120*, 6625.
(19) Max, J.-J.; Chapados, C. *J. Chem. Phys.* **2005**, *122*, 014504.
(20) Max, J.-J.; Chapados, C. *J. Chem. Phys.* **2001**, *115*, 2664.
(21) Max, J.-J.; Chapados, C. *J. Chem. Phys.* **2002**, *116*, 4626.
(22) Zelsmann, H. R. *J. Mol. Struct.* **1995**, *350*, 95.
(23) Weast, R. C. *Handbook of Chemistry and Physics*, 57th ed.; CRC Press: Cleveland, OH, 1976.
(24) Max, J.-J.; Chapados, C. *J. Chem. Phys.* **2000**, *113*, 6803.
(25) Max, J.-J.; de Blois, S.; Veilleux, A.; Chapados, C. *Can. J. Chem.* **2001**, *79*, 13.
(26) Iawata, T.; Koshoubu, J.; Jin, C.; Okubo, Y. *Appl. Spectrosc.* **1997**, *51*, 1269.
(27) Max, J.-J.; Chapados, C. *Can. J. Anal. Sci. Spectrosc.* **2002**, *47*, 72.
(28) Max, J.-J.; Daneault, S.; Chapados, C. *Can. J. Chem.* **2002**, *80*, 113.
(29) Kodad, H.; Mokhlisse, R.; Davin, E.; Mille, G. *Can. J. Appl. Spectrosc.* **1994**, *39*, 107.
(30) The sample compositions are calculated from the volume of water and carbohydrate masses. From data in ref 24, we derived the numerical relationship between carbohydrate concentration and water concentration as a function of carbohydrate molar fraction χ. These are, respectively for D-glucose and D-fructose [D-glucose] $= 0.9614\chi^3 + 1.9904\chi^2 + 5.5584\chi - 0.0005$ and $[H_2O] = -9.6147\chi^2 - 33.0182\chi + 55.3410$; [D-fructose] $= 0.9032\chi^3 + 2.1045\chi^2 + 5.5466 \times c - 0.0001$ and $[H_2O] = -21.3070\chi^2 - 31.9004\chi + 55.3064$. Error resulting from the polynomial fitting was less than ± 0.1 mM.
(31) The molar relative intensities of a sample with carbohydrate concentration c_s was simply obtained by integrating the absorbance $I^{OH}_{rel}(c_s) = (\int_{3000}^{3700} I^{OH}_{c_s} d\tilde{\nu} / \int_{3000}^{3700} I^{OH}_{0} d\tilde{\nu}) \times (2c_w(0)/(2c_w(c_s) + 5c_s))$ for the O_h stretch band and $I^{HOH}_{rel}(c_s) = (\int_{1550}^{1750} I^{HOH}_{c_s} d\tilde{\nu} / \int_{1550}^{1750} I^{HOH}_{0} d\tilde{\nu}) \times (c_w(0)/c_w(c_s))$ for the HOH deformation band were $c_w(0)$ is the water concentration in pure liquid and $c_w(c_s)$ is the water concentration at carbohydrate concentration c_s. The 3000 cm^{-1} lower limit for the OH intensity was determined to avoid contribution from the sugar CH bands. The lower limit at 1550 cm^{-1} for water ν_2 integration had been selected to coincide to the minimum of the absorption intensity of the highest concentration of the sugar solution (Figures 1 and 2). No baseline removal was performed.
(32) Along with the new **MF′**, the principal factor spectra are recalculated according to $(\mathbf{S^{P'}})_{f,l} = (\mathbf{S^P})_{l,f} \times [(\mathbf{P'}) \times (\mathbf{P})^{-1}]$, ref 18.
(33) Relating both constants to a similar unit, $L \times mol^{-1}$ gives, $\sqrt{K_F} = 8.4 \times 10^{-2}$ L mol^{-1} and $\sqrt[3]{K_G} = 3.2 \times 10^{-2}$ L mol^{-1}.